

Supplementary Information for Manuscript_VAADIA

Supplementary Results

Relation of speed on behavioral and neuronal findings

Movement duration in the pre-learning null-field trials was on average ~385 ms for both feedback conditions (Supplementary Table 1). Early in force-field adaptation, monkeys took more time to reach the target (increase by 13% with VFB and 22% without VFB). However, with practice, movement times under force-field were only 7-9% longer than pre-learning movement times. Thus, it could be argued that monkeys might have reduced directional deviations by reducing speed. However, the following results show that this is unlikely. First, reduction of directional deviations did not correlate with speed (Pearson's correlation $P > 0.10$). Second, a strategy that relied on slowing down would not produce the directional aftereffects we had observed in catch-trials (Fig. 1C-D). Lastly, delaying the time to peak velocity may imply a reliance on feedback-mediated corrections. However, the time to peak velocity in the late force-field trials did not reflect a shift to a feedback control policy (Supplementary Table 1).

Speed of arm movements has been found to also modulate the firing of motor cortical cells (Schwartz, 1992;Fu et al., 1993;Johnson et al., 1999;Moran and Schwartz, 1999;Reina et al., 2001). In this present study, peak velocities in null-field reaches were 30% higher than peak velocities in field reaches late in adaptation (Supplementary Table 1). Such difference might explain the observed changes in neuronal activity. Specifically, the observed decrease in firing rates found in cells with PDs along the direction where force-field assists movement (see Figure 5) might be due to speed reduction. Although this was unlikely for the reasons stated above, we verified whether those cells that decreased their activity still did so when monkeys moved fast under force-field (i.e. "fast trials" defined as trials with peak velocity of greater than 100% of the unperturbed baseline trials). Analysis using only fast trials still yielded significant decreases in firing rates for those same cells

that showed reduced firing rates when all trials were analyzed (Supplementary Fig. 3B, Mann Whitney $P < 0.05$). Thus, these results imply that the decrease in firing rates during force-field adaptation could not be ascribed mainly to speed reduction. Furthermore, the concordance between the directional after-effects and the direction of the population vector supports that speed reduction do not account primarily for the pattern of rate modulation observed here.

Supplementary Discussion

Inferring generalization patterns from model predictions

We made predictions on the generalization patterns based on the adaptive modulation profile of neurons modulated by force-field and verified them against the reported generalization patterns of force-field adaptation in humans. Supplementary Figure 3 illustrates the predicted generalization patterns. Because the mean positive and negative modulations corresponded to the counter-field and with-field cells respectively, we took these two groups of cells to represent the population. We assumed that the generalization to a specific direction to be proportional to changes in firing rates in that same direction (Supplementary Fig. 4A gray-shaded area) such that increases would underlie positive transfer and decreases do not. This assumption was partly based on previous study where cells with PD near the learned hand direction retained the increased activity even with the cessation of the visuomotor rotation (Paz *et al.*, 2003). As mentioned in the Results section, we also found here that 29% of the force-field modulated cells retained their adaptive changes through the post-learning block.

Generalization of force-field adaptation has been suggested to be limited to directions near the trained direction (Gandolfo *et al.*, 1996; Thoroughman and Shadmehr, 2000; Donchin *et al.*, 2003; Mattar and Ostry, 2007). While all these studies agree that positive transfer occurs maximally at the learned direction and decays as a function of angular separation, there is disagreement over interference

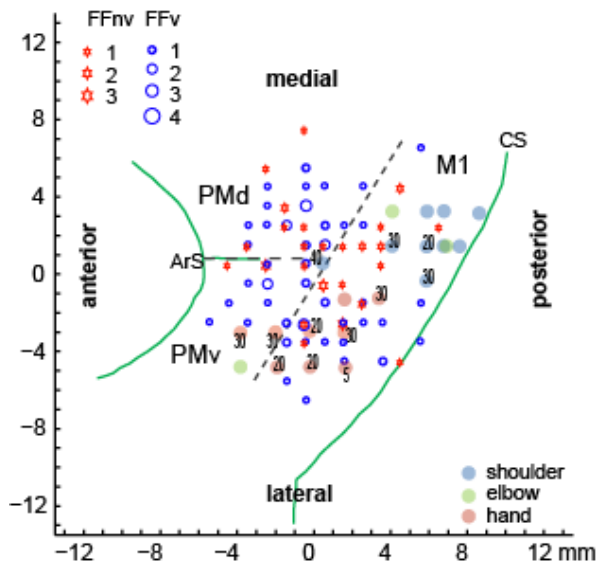
for directions beyond $\pm 90^\circ$. Our model shows that these contrasting views may be accounted for by the differences in the number of training directions (one vs. eight) and how transfer is tested (null-field vs. force-field reaches). For **local learning**, our model predicts transfer to **null-field reaches** to be maximal at the LD and to decay away from it, proportional to the graded increase predicted by the cosine model for CF cells (Supplementary Fig. 4B). Since learning is local, no transfer is expected for directions where firing rates decrease for the CF cell. This explains the lack of transfer beyond $\pm 90^\circ$ reported by (Mattar and Ostry, 2007). By contrast, our model predicts maximal interference opposite to the LD when transfer is tested with **force-field** because the required modulation would be the reverse of the previously learned modulation. Thus, CF and WF cells would fire as learned previously for movements to the LD to signal a leftward compensatory force when the required one was rightward. This explains the interference reported by (Thoroughman and Shadmehr, 2000; Donchin et al., 2003), as well as the observed interference when learning opposing force-fields (Shadmehr and Brashers-Krug, 1997; Caithness et al., 2004).

For **8-target learning** (Supplementary Fig. 4C), our model predicts maximal transfer in two opposing directions corresponding to the peak positive modulation at 0° and 180° of CF and WF cells, respectively, while minimal transfer corresponds to directions with minimal positive modulation at 90° and -90° . Note also the asymmetry of transfer between 45° vs. -45° and 135° vs. -135° , accounted for by the increasing modulation as the distance between the PD and the LD approximates the PD of the population response at -100° (see Fig. 6A). Our predictions conform to that reported by (Donchin *et al.*, 2003). Our model however does not predict interference but rather positive transfer in directions $\pm 90^\circ$ away from the LD for 8-target learning. As the expected force approximates the required force with practice, successive trials to targets separated by $\pm 90^\circ$ would no longer interfere

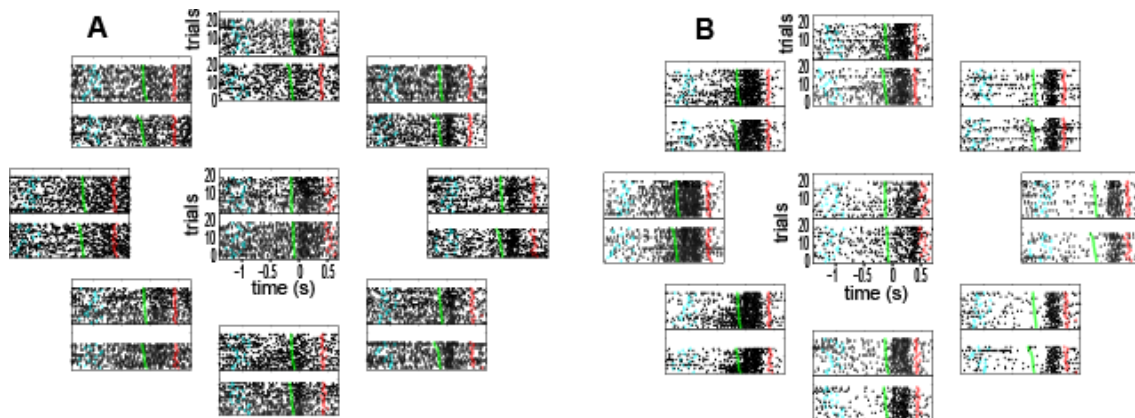
each other. This means that eventually CF and WF cells would have learned how to fire appropriately for all 8 directions.

Psychophysical studies also reported limited generalization of force-field adaptation with postural changes when the workspace was moved up to 80 cm away from the training workspace (Shadmehr and Moussavi, 2000; Malfait et al., 2002). Our model for neuronal activity predicts this generalization pattern. It is plausible that PDs would shift as the shoulder rotates with the change of workspace (Caminiti et al., 1990). The extent of generalization depends on the difference between the PD after training (Supplementary Fig. 4D₁) and the PD prior to transfer test (Supplementary Fig. 4D₂₋₃). If PDs shift such that CF cell reverses its modulation from positive to negative (and vice-versa for WF cell), we predict lack of transfer (Supplementary Fig. 4D₂). Otherwise, transfer is expected to occur (Supplementary Fig. 4D₃) in those directions where the new predicted modulation matches the previously learned modulation. The same mechanism underlies transfer to the other arm (Criscimagna-Hemminger et al., 2003). Since M1 and dorsal PM cells have been shown to be directionally tuned with both arms and with similar PDs (Steinberg et al., 2002; Cisek et al., 2003), our results predict transfer if the neural elements that were modulated previously when adapting with one arm are also tuned for movements of the other arm.

Supplementary Figures

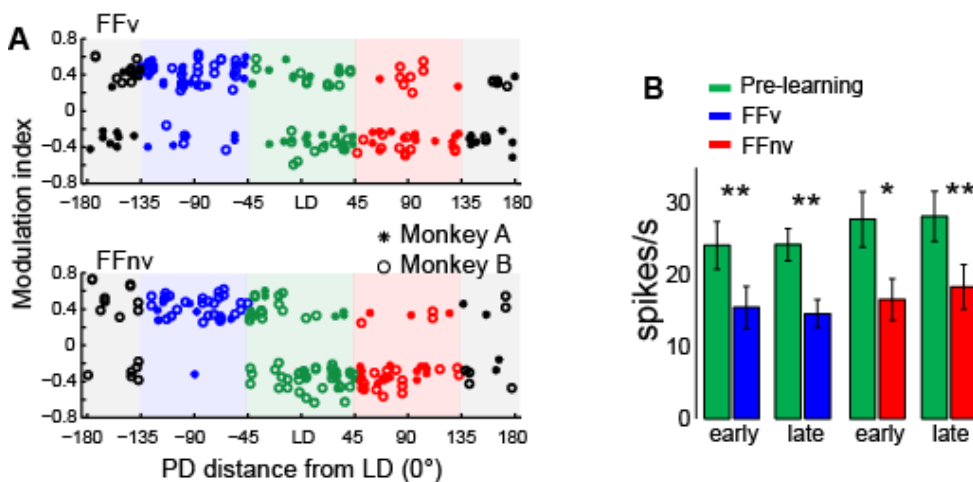


Supplementary Figure 1. Cortical surface map of monkey A. The figure shows penetration sites where force-field modulated neurons (in FFv and FFnv) were found. Modulated cells were found in primary motor (M1), dorsal (PMd) and ventral (PMv) premotor cortices (see Supplementary Table 2). Marker size corresponds to the number of cells that were recorded on a site. Filled colored circles correspond to sites where arm responses were elicited by microstimulation of $<40 \mu\text{A}$ or passive limb movement. Dashed lines correspond to estimated divisions between motor cortical areas based on bone surface landmarks, MRI analyses and microstimulations. CS=central sulcus; ArS=arcuate sulcus.

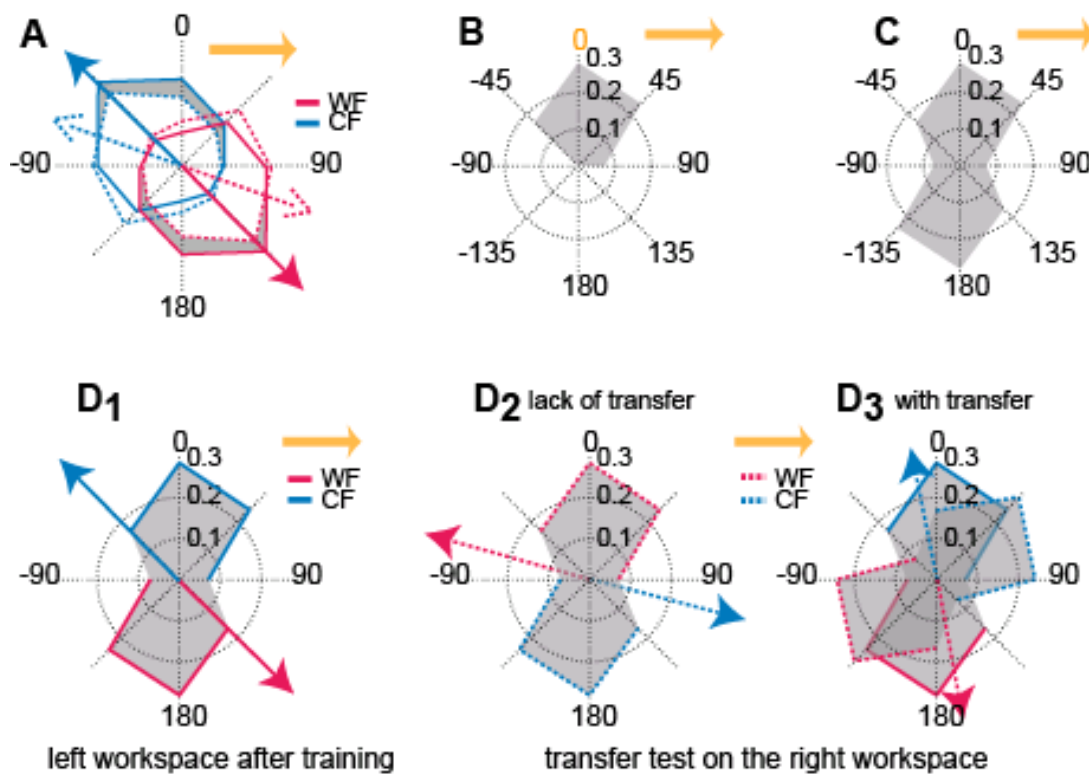


Supplementary Figure 2. Raster plots of the same cells shown in Figure 4.

Raster plots for movements to eight directions during pre- (lower rectangle) and post-learning (upper rectangle) blocks. Raster plots in the center correspond to early (lower) and late (upper) trials of force-field. Activity is aligned at movement onset (0 s) and colored dots correspond to the time of the following events: target-onset (cyan), go-signal (green), and movement-end (red). Shown for the same cells in Figure 4A-B.



Supplementary Figure 3. A, Modulation indexes during adaptations to FFv and FFnv, shown separately for each monkey and plotted according to the distance between their preferred directions (PD) and the learned direction (LD). **B**, Mean firing rates in pre-learning unperturbed trials and in "fast" force-field trials for cells that showed negative modulation during adaptations to force-fields. Error bars: ± 1 SE. **= $P \leq 0.01$, *= $P < 0.05$.



Supplementary Figure 4. Patterns of force-field generalization as explained by the cosine-tuned modulation. **A**, Polar plots of actual and predicted firing rates in pre-learning (dashed) and force-field (solid) blocks, shown for CF and WF cells. For a clockwise force-field, a CF cell increases its firing rate for target directions $\pm 45^\circ$, 90° , and maximally at 0° . For these same directions, a WF cell decreases activity in a graded manner as well. By contrast, for directions -90° , $\pm 135^\circ$, 180° , a WF cell increases firing while CF cell decreases firing. Note that for these latter directions, WF cell actually becomes a CF cell (and vice versa) as the relation of their PDs to these directions reverses. Arrows represent the PDs of these cells in the corresponding blocks. Gray-shaded areas correspond to directions where firing rates increased from pre-learning to force field. Orange arrow denotes direction of force-field. **B**, Predicted generalization after local learning. Polar plot of the positive modulation indexes of CF cell (-45° - 90°). LD at 0° . **C**, Predicted

generalization after 8-target learning. Polar plot of the positive modulation indexes of CF (-45° : 90°) and WF (-90° : 135°) cells. **D**, Generalization to other workspace. ***D*₁**, Modulation indexes and PDs (solid arrows) corresponding to CF and WF cells after training on the left workspace. ***D*₂₋₃**, Transfer tests on the right workspace. The PDs prior to transfer test (dashed arrows) result from the PD acquired after previous training plus (possible) shoulder rotation due to the change of workspace location. ***D*₂**, Illustration of lack of transfer: If change of workspace location induces PDs to shift such that CF cell reverses its modulation from positive to negative and vice-versa for the WF cell, we predict lack of transfer. ***D*₃**, Illustration of transfer: The extent of the transfer is constrained to those directions where the predicted modulation (dashed) matches the learned modulation (solid).

Supplementary Table 1. Means and standard errors (± 1) of behavioural parameters.

Parameters	Pre-learning		Early adaptation		Late adaptation	
	FFv	FFnv	FFv	FFnv	FFv	FFnv
Distance (mm)	39.8 \pm 3.8	40.6 \pm 3.7	40.6 \pm 4.0	40.8 \pm 3.8	38.9 \pm 3.3	39.5 \pm 3.5
Duration (ms)	385 \pm 107	386 \pm 110	436 \pm 108	474 \pm 96	411 \pm 119	420 \pm 109
Peak velocity (m/s)	0.17 \pm 0.04	0.18 \pm 0.04	0.13 \pm 0.03	0.12 \pm 0.03	0.13 \pm 0.06	0.14 \pm 0.03
Peak velocity time (ms)	181 \pm 69	184 \pm 66	292 \pm 100	310 \pm 118	267 \pm 100	260 \pm 105
Reaction time (ms)	237 \pm 75	228 \pm 74	237 \pm 78	228 \pm 72	232 \pm 76	216 \pm 62
Success rates	94 \pm 2	79 \pm 7	89 \pm 3	65 \pm 4	92 \pm 3	77 \pm 5

Supplementary Table 2. Proportion of force-field modulated cells according to cortical location. Over 73% (314/428) of the cells recorded from monkey-A were directionally tuned (bootstrap $P < 0.05$), of which 32% (100/314) showed significant modulation by force-field.

Motor areas	FFv (n=63/180)	FFnv (n=37/134)
M1	23/89 (26%)	23/66 (35%)
PMd	25/68 (37%)	9/57 (16%)
PMv	15/23 (65%)	5/11 (45%)

Reference List

Caithness G, Osu R, Bays P, Chase H, Klassen J, Kawato M, Wolpert DM, Flanagan JR (2004) Failure to consolidate the consolidation theory of learning for sensorimotor adaptation tasks. *J Neurosci* 24:8662-8671.

Caminiti R, Johnson PB, Urbano A (1990) Making Arm Movements Within Different Parts of Space: Dynamic Aspects in the Primate Motor Cortex. *J Neurosci* 10:2039-2058.

Cisek P, Crammond DJ, Kalaska JF (2003) Neural Activity in Primary Motor and Dorsal Premotor Cortex In Reaching Tasks With the Contralateral Versus Ipsilateral Arm. *J Neurophysiol* 89:922-942.

Criscimagna-Hemminger SE, Donchin O, Gazzaniga MS, Shadmehr R (2003) Learned Dynamics of Reaching Movements Generalize From Dominant to Nondominant Arm. *J Neurophysiol* 89:168-176.

Donchin O, Francis JT, Shadmehr R (2003) Quantifying generalization from trial-by-trial behavior of adaptive systems that learn with basis functions: theory and experiments in human motor control. *J Neurosci* 23:9032-9045.

Fu QG, Suarez JI, Ebner TJ (1993) Neuronal specification of direction and distance during reaching movements in the superior precentral premotor area and primary motor cortex of monkeys. *J Neurophysiol* 70:2097-2116.

Gandolfo F, Mussa-Ivaldi FA, Bizzi E (1996) Motor learning by field approximation. *Proc Natl Acad Sci U S A* 93:3843-3846.

Johnson MT, Coltz JD, Ebner TJ (1999) Encoding of target direction and speed during visual instruction and arm tracking in dorsal premotor and primary motor cortical neurons. *Eur J Neurosci* 11:4433-4445.

Malfait N, Shiller DM, Ostry DJ (2002) Transfer of motor learning across arm configurations. *J Neurosci* 22:9656-9660.

Mattar AAG, Ostry DJ (2007) Modifiability of Generalization in Dynamics Learning. *J Neurophysiol* 98:3321-3329.

Moran DW, Schwartz AB (1999) Motor cortical representation of speed and direction during reaching. *J Neurophysiol* 82:2676-2692.

Paz R, Boraud T, Natan C, Bergman H, Vaadia E (2003) Preparatory activity in motor cortex reflects learning of local visuomotor skills. *Nat Neurosci* 6:882-890.

Reina GA, Moran DW, Schwartz AB (2001) On the relationship between joint angular velocity and motor cortical discharge during reaching. *J Neurophysiol* 85:2576-2589.

Schwartz AB (1992) Motor cortical activity during drawing movements: single-unit activity during sinusoid tracing. *J Neurophysiol* 68:528-541.

Shadmehr R, Brashers-Krug T (1997) Functional stages in the formation of human long-term motor memory. *J Neurosci* 17:409-419.

Shadmehr R, Moussavi ZM (2000) Spatial generalization from learning dynamics of reaching movements. *J Neurosci* 20:7807-7815.

Steinberg O, Donchin O, Gribova A, Cardoso dO, Bergman H, Vaadia E (2002)
Neuronal populations in primary motor cortex encode bimanual arm movements.
Eur J Neurosci 15:1371-1380.

Thoroughman KA, Shadmehr R (2000) Learning of action through adaptive
combination of motor primitives. Nature 407:742-747.